BJRS

BRAZILIAN JOURNAL
OF
RADIATION SCIENCES
07-2A (2019) 01-13

X-ray diffraction analysis of KY_3F_{10} nanoparticles doped with Nd and preliminary studies for its use in high-dose radiation dosimetry

R. U. Ichikawa[a]; H. M. S. M. D. Linhares[b]; A. S. B. da Silva[a]; M. I. Teixeira[a]; I. M. Ranieri[a]; X. Turrillas[c,d]; L. G. Martinez[a]

[a] *Instituto de Pesquisas Energéticas e Nucleares, Av. Prof. Lineu Prestes-2242, 05508-000, São Paulo, SP, Brazil*

[b] *Universidade Federal Fluminense, Av. João Jasbick, s/nº, 28470-000, Santo Antônio de Pádua, RJ. Brazil*

[c] *Institut de Ciència de Materials de Barcelona, UAB Campus, 08193 Bellaterra, Barcelona, Spain*

[d] *ALBA Synchrotron, Carrer de la Llum, 2-26, 08290 Cerdanyola del Vallès, Barcelona, Spain*

ichikawa@usp.br

ABSTRACT

In this work, the structure and microstructure of Nd:KY_3F_{10} nanoparticles was probed using X-ray synchrotron diffraction analysis. Rietveld refinement was applied to obtain cell parameters, atomic positions and atomic displacement factors to be compared with the ones found in literature. X-ray line profile methods were applied to determine mean crystallite size and crystallite size distribution. Thermoluminescent (TL) emission curves were measured for different radiation doses, from 0.10 kGy up to 10.0 kGy. Dose-response curves were obtained by area integration beneath the peaks from TL. The reproducibility of the results in this work has shown that this material can be considered a good dosimetric material.

Keywords: X-ray diffraction, thermoluminescence, KY_3F_{10}, nanoparticles.

ISSN: 2319-0612
Accepted: 2018-12-10

1. INTRODUCTION

With the advent of nanoscience and nanotechnology the study of materials that exhibits properties to be applied in different areas is very interesting. This is the case of KY_3F_{10} nanoparticles, which has a cubic symmetry with nonequivalent sites for rare-earth ions [1]. This material can be doped with different rare-earth atoms such as Yb, Tm, Nd [2] and Yb, Er [3], that make this material interesting for luminescent applications [2,3].

Besides that, there is an interest to produce luminescent materials to be used as radiation detectors and solid state dosimeters in various areas for industrial, scientific and medical applications [4]. For this application, fluoride compounds are widely studied [4,5] for its interesting thermoluminescent properties. Thermoluminescence (TL) is a simple and widely used technique for radiation dosimetry. The intensity of the light emitted by the dosimetric material is proportional to the radiation doses applied and can be quantified when a calibration is established from known doses. The incident radiation, when interacting with the crystalline lattice, is absorbed and its energy creates defects in the structure of the material, as for example, atomic displacements or electron trapping in vacancies. Upon heating, these defects are extinguished and the energy previously acquired for their formation is released in the form of light, which is detected and quantified. The result is an intensity versus temperature curve, which means that the thermoluminescent signal is dependent on the temperature of the heat applied to the irradiated material and the position of the thermoluminescent emission peaks are directly related to the energy of the defects created.

The dosimetric technique based on optically stimulated luminescence (OSL) consists in detecting the light emission from a dosimetric material, after having been irradiated, when excited with appropriate wavelengths. This is possible when the dosimetric material has metastable levels of impurities or dopants in the conduction band, which act as traps for photoexcited electrons and/or holes. The OSL signal is a decay curve proportional to the release of the trapped electrons in the point defects of the lattice created by the irradiation (X-rays, gamma, alpha or beta) [6,7].

In this work, KY_3F_{10} doped with Nd (Nd:KY_3F_{10}) synthesized using coprecipitation, that was already investigated by Linhares [8] for luminescent applications, was studied for high-dose radiation dosimetry applications. Our results show that the material can be used for dosimetric applications

with a coefficient of variation of approximately 7.71 %. Also, X-ray diffraction data was collected using synchrotron radiation for structural and microstructural analysis. Results from Rietveld refinement reveal that the material does not present major structural deviations with refined parameters close to the ones reported in the literature. The Warren-Averbach [9] method was applied for mean crystallite size and microstrain estimations revealing a broad crystallite size distribution around approximately 3 nm with very low microstrain.

2. MATERIALS AND METHODS

The KY_3F_{10} nanoparticles doped with Nd (1.3 mol%) were synthesized using coprecipitation, as described in detail in a previous work [2].

A pellet of 50 mg (proportion of 2:1, Teflon:KY_3F_{10}) with 6 mm of diameter and 2 mm of thickness was obtained under 2 tons of load at the Dosimetric Materials Production Laboratory of IPEN. The pellet was then irradiated at the Radiation Technology Center of IPEN, using a Gamma-Cell 220 - ^{60}Co system with a dose rate of 1.258 kGy/h, from 0.10 kGy up to 10.0 kGy doses.

Thermoluminescence (TL) measurements were performed at ambient temperature up to 300 ºC using an equipment RISÖ TL/OSL Reader and Controller, model DA-20. During the acquisition a constant N_2 flux of 2.5 L/min, with U340 filter and heating rate of 10 °C/s was maintained. Optically stimulated luminescence (OSL) measurements were performed in the same equipment. It was used a set with 28 LED (light emitting diodes) as light source. This set can emit at 470 nm delivering 80 mW/cm^2 [10].

The synchrotron radiation measurements were performed at the Brazilian Synchrotron Light Laboratory (*Laboratório Nacional de Luz Síncrotron* – LNLS, in Portuguese) in the XRD1 beamline. The powdered sample was introduced in 0.8 mm borosilicate capillaries and kept rotating during data acquisition. A wavelength of 1.033305 Å was used.

X-ray diffraction analysis was performed using Rietveld and Warren-Averbach [9] methods. Rietveld analysis is a very complex curve fitting problem which basically parametrizes the crystal structure and the diffraction experiment [11]. The experimental diffraction data is fitted using a least-squares procedure which minimizes the difference between the experimental data and the cal-

culated model. With this, reliable structural parameters can be obtained such as cell parameters, atomic displacement factors, atomic positions, occupancies, etc. Also, microstructural parameters (mean crystallite size and microstrain) can be obtained refining first a standard reference material to correct the instrumental contribution. Rietveld method was applied refining 15 background coefficients (fitted using a Chebyshev polynomial), cell parameters, atomic positions, atomic displacement factors. Volume-weighted mean crystallite size ($\langle L \rangle_V$) and microstrain were refined using a macro from the software TOPAS 4.2 [12] based on the work of Balzar et al. [13,14].

However, for a more rigorous calculation of mean crystallite size and microstrain, Warren-Averbach (W-A) method is still the most unbiased method for this type of analysis. W-A method uses the Fourier coefficients obtained from the Fourier Transform of the diffraction peak profile to estimate the area-weighted mean crystallite size and root mean square strain from two parallel reflections. For a detailed description and definition of mean crystallite sizes and microstrains used in this work the reader is encouraged to read reference [15].

3. RESULTS AND DISCUSSION

The X-ray diffraction profile correspond to a cubic structure (Space Group, $Fm\bar{3}m$, No. 225), the observed reflections (black vertical lines) can be seen in Fig. 1. The Rietveld refinement can be seen in Fig. 1 and the results were summarized in Table 1.

Figure 1: *Rietveld refinement for the Nd:KY_3F_{10} sample. Vertical black lines represent the* (*hkl*) *reflections. In the inset, the refinement for higher angles (75° up to 120°).*

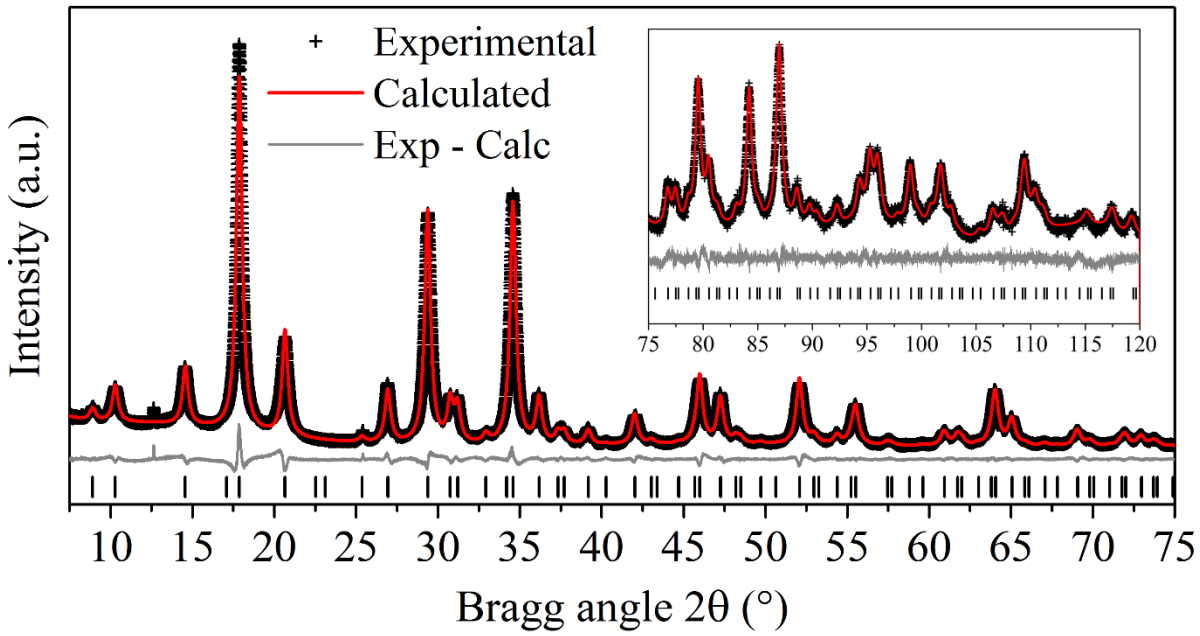

Table 1: Rietveld refinement results for cell parameter (a), atomic positions (x,y,z), atomic displacement factors (B), volume-weighted mean crystallite size ($\langle L \rangle_V$) and maximum strain (e_0).

Parameter	Value
a (Å)	11.53415 (12)
x Y	0.24134 (4)
x,y,z F1	0.11334 (9)
y,z F2	0.16546 (7)
U Y (Å^2)	0.0065 (1)
U K (Å^2)	0.0254 (5)
U F1 (Å^2)	0.0096 (4)
U F2 (Å^2)	0.0165 (4)
$\langle L \rangle_V$ (nm)	10.2 (1)
e_0	0.04 (1)

In the refinements, the cation Nd was added sharing the position with Y cation, but no improvement in the refinement was observed, this is probably due to the small amount of doping (1.3 mol%). So, the occupation of Y was kept as one and Nd removed from the refinement. The calcu-

lated parameters are in good agreement with the ones reported in the work of Grzechnik et al. [16] (a = 11.553 (1) Å). Cell parameters and atomic positions differences are no greater than 1.4 %. Main differences lie in the atomic displacement factors, this is most likely due to differences in the samples. Grzechnik et al. performed the study using a single crystal while this work is on nanostructured polycrystals. The main difference is for the Fluorine anion that present a difference up to 66.9 % in the atomic displacement factor, when compared with the ones from the literature, however this is expected since F is a very light atom. The volume-weighted mean crystallite size around 10 nm confirm that nanosized particles were successfully synthesized, although it needs to be confirmed with W-A method, although this can be used as an initial estimation. The maximum strain value (as defined by Balzar [14]) is relatively low showing that the nanoparticles present very low microstrain.

For a more rigorous microstructural characterization, Warren-Averbach method was applied according with the procedure described in reference [17]. An area-weighted mean crystallite size ($\langle L \rangle_A$) of 5.3 nm was found with a root mean square strain of 0.0009, which is an almost negligible microstrain, in agreement with the one found by Rietveld. With $\langle L \rangle_A$ and $\langle L \rangle_V$, the size distribution assuming spherical crystallites and the lognormal function can be obtained. The distribution yielded a mean value of 2.7 nm and a standard deviation 2.3 nm, which can be considered a broad distribution. These combined values of $\langle L \rangle_A$ and $\langle L \rangle_V$ confirm the nanometer scale of the synthesized particles. These results are shown graphically in Fig. 2.

Figure 2: *Warren-Averbach size coefficients (empty black line-dots) for the determination of the area-weighted mean crystallite size ($\langle L \rangle_A$=5.3 nm). $\langle L \rangle_A$ is determined from the linear fit (red line) intercept with x-axis. In the inset, the crystallite size distribution (black line-dots) is presented in conjunction with the cumulative distribution (blue line-dots).*

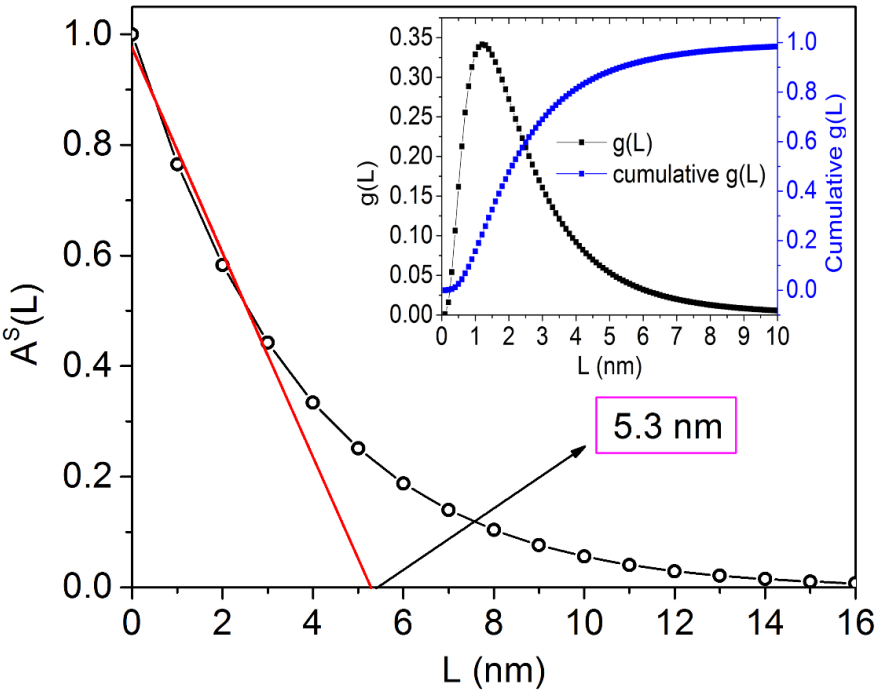

The TL emission curves for different doses were measured in a range of 0.10 kGy and 50 kGy (Fig. 3). The curves present two main peaks: one approximately at 180°C which increases in intensity up to 5 kGy and abruptly decreases for high doses (Fig. 3a). The second peak at approximately 250 °C increases in the same proportion with the radiation dose. Normalizing the intensity of the curves, the one at 10 kGy presents a broadening at approximately 250 °C. Apparently, there is the formation of a third center, which may be formed by the peaks at 180 °C.

Figure 3: *Nd:KY_3F_{10} nanocrystal TL emission curves for: (a) 0.1, 0.5, 1.0, 5.0 and 10.0 kGy doses; (b) same curves normalized.*

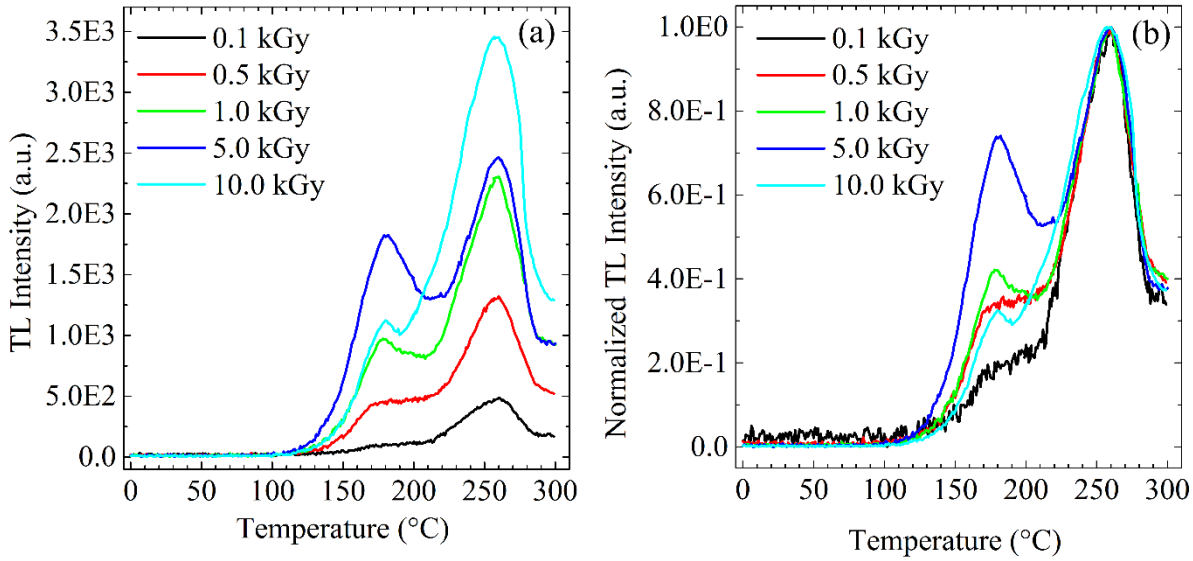

Deconvoluting the curves using Gaussian functions it can be seen that the curves are the convolution of 2 functions for the 0.1 up to 5 kGy TL curves. In Fig. 4a where the 1 kGy TL curve is presented, the first peak is centered at 179 °C and the second at 256 °C. The 10 kGy TL curve (Fig. 4b) is composed of three Gaussian functions centered at 179 °C, 213 °C and 256 °C. For the 10kGy irradiated sample, the peak at 179 °C is less intense since the curves present the convolution of three peaks (179 °C, 213 °C and 256 °C), so the first peak at 179 °C is less intense compared to 0.5 kGy, 1.0 kGy and 5.0 kGy due to the presence of the second peak at 213 °C. If we sum the energies for the first and second peaks we have an energy with higher intensity.

Figure 4: *TL emission curve deconvolution for the Nd:KY_3F_{10} nanopowder obtained for doses of: (a) 1 and (b) 10 kGy.*

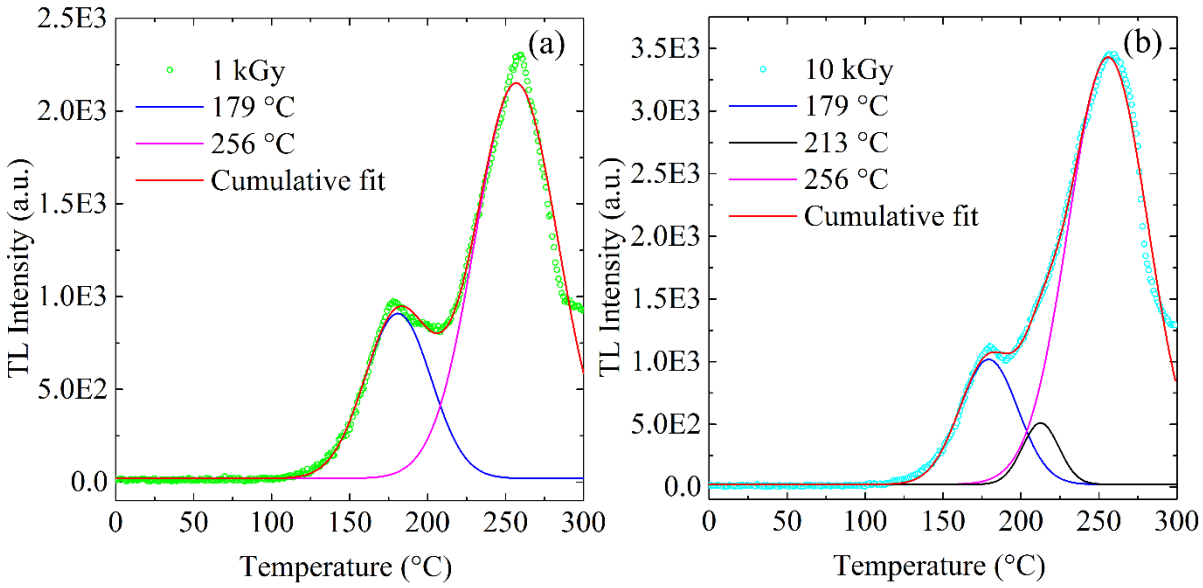

The OSL curve was obtained for two doses to verify if it could be used as an alternative for TL system. However, the signal was not intense when the sample was excited. This indicates that energy of the excitation light was not sufficient to stimulate metastable charges trapped in the defects produced by ^{60}Co gamma radiation (Fig. 5).

Figure 5: *(a) OSL curve for Nd:KY_3F_{10} nanocrystal. (b) Dose-response TL curves (integrated area) of Nd:KY_3F_{10}.*

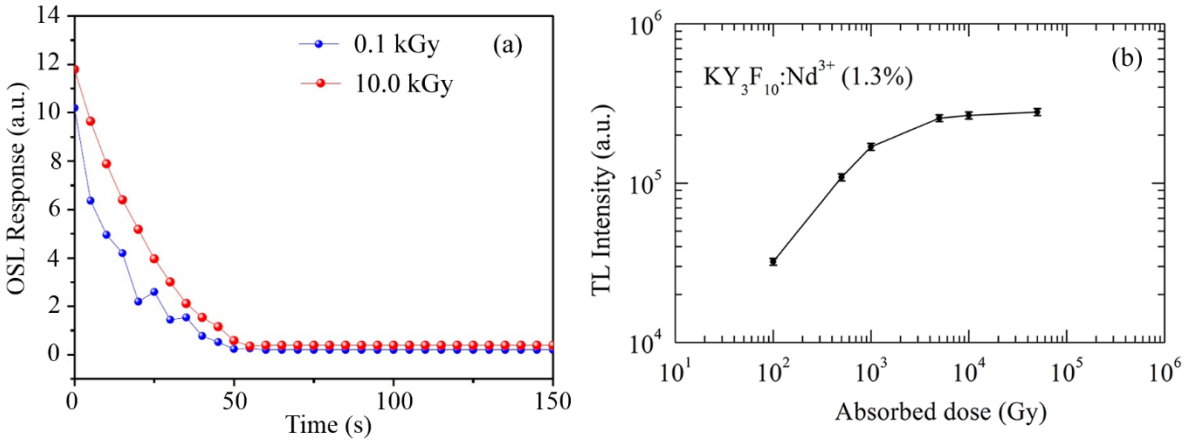

The determination of the dose-response curve for this material was obtained by integration of the area underneath the TL curves. It can be observed that the curve presents a sub linearity and a saturation from 5 kGy (Fig. 5) with maximum relative standard deviation of 2.3 %. However, new experiments are necessary to verify the behavior of the material when irradiated with lower doses.
The lower detection limit of the samples in this experiment is 8.0 kGy and was determined by studying the variability of the TL signal obtained from samples treated at 300 °C/1h but not irradiated. Taking three times the standard deviation of these measurements, the lower detection limits (8 kGy) [18].
The reproducibility of the results in this experiment is given by the coefficient of variation (CV), defined as the ratio between the standard deviation and the mean of the measurements. For the Nd:KY_3F_{10} the CV was 7.71 % making it suitable for dosimetric applications since the maximum CV for this purpose must be lower than 10.0%.

4. CONCLUSION

In this work, Nd:KY_3F_{10} nanoparticles were analyzed using X-ray diffraction (XRD), Thermoluminescence (TL) and Optically Stimulated Luminescence (OSL) methods. The XRD profile was successfully refined using a cubic structure (S.G. $Fm\bar{3}m$, No. 225) and the values are in good accordance with the ones reported in the literature. Warren-Averbach method confirmed that nanosized particles were synthesized and allowed the calculation of the size distribution, which revealed that the nanoparticles are quite dispersed around 2 nm. Additionally, W-A method showed that no appreciable microstrain is present. The TL emission curves measured at 0.1 and 5.0 kGy presented the formation of two centers at 179 °C and 256 °C, while the one measured at 10 kGy is composed of three centers at 179 °C, 213 °C and 256 °C. As an alternative, the OSL curve was obtained for two radiation absorbed doses. However, the signal was not sufficiently intense to stimulate metastable charges trapped in the defects produced by radiation. Finally, the coefficient of variation (CV) allowed to conclude that the material can be used for dosimetric purposes with a CV of 7.71 %.

5. ACKNOWLEDGMENT

The authors acknowledge LNLS and XRD1 beamline staff for the synchrotron radiation measurements and support during the experiment. RUI and ASBS acknowledge CAPES and CNPq (No. 206983/2014-0) for the financial support.

REFERENCES

1. CHAMBERLAIN, S. L.; CORRUCCINI, L. R. Magnetic ordering in rare-earth fluorides with KY_3F_{10} structure and axial moments. **Phys Rev B**, v. 71, p. 024434-1-7, 2005.

2. GOMES, L.; LINHARES, H. M. S. M. D.; ICHIKAWA, R. U.; MARTINEZ, L. G.; RANIERI, I. M. Luminescence properties of Yb:Nd:Tm:KY_3F_{10} nanophosphor and thermal treatment effects. **J Lumin**, v. 157, p.285–292, 2015.

3. GOMES, L.; LINHARES, H. M. S. M. D.; ICHIKAWA, R. U.; MARTINEZ, L. G.; BALDOCHI, S. L. Luminescence properties of Yb:Er:KY_3F_{10} nanophosphor and thermal treatment effects. **Opt Mater**, v. 54, p. 57-66, 2016.

4. KUI, H. W.; LOA, D.; TSANG, Y. C.; KHAIDUKOV, N. M.; MAKHOV, V. N. Thermoluminescence properties of double potassium yttrium fluorides singly doped with Ce^{3+}, Tb^{3+}, Dy^{3+} and Tm^{3+} in response to α and β irradiation. **J Lumin**, v. 117, p. 29-38, 2006.

5. KRISTIANPOLLERA, N.; WEISSA, D.; KHAIDUKOVB, N.; MAKHOVC, V.; CHENA, R. Thermoluminescence of some Pr^{3+} doped fluoride crystals. **Radiat Meas**, v. 43, p. 245-248, 2008.

6. NAVARRO, M. S.; LIMA, J. F.; VALERIO, M. E. G. Effects of thermal treatments on the TL emission of natural quartz, **Radiat Meas**, v. 35, p. 155-159, 2002.

7. TEIXEIRA, M. I.; SOUZA, D. N.; CALDAS, L. V. E. Onyx as radiation detector for high doses. **Radiat Meas**, v. 46, p. 1894-1896, 2011.

8. LINHARES, H. M. S. M. D. Síntese de nanocristais de KY_3F_{10} pelo método de co-precipitação visando aplicações ópticas. Tese de Doutorado em Tecnologia Nuclear – Materiais. Instituto de Pesquisas Energéticas e Nucleares, Universidade de São Paulo, São Paulo (2014).

9. WARREN, B. E.; AVERBACH, B. L. The Effect of Cold-Work Distortion on X-Ray Patterns. **J Appl Phys,** v. 21, p. 595-599, 1950.

10. GROPPO, D. P.; CALDAS, L. V. E. OSL response bleaching of BeO samples, using fluorescent light and blue LEDs. **J Phys Conf Ser**, v. 733, p. 012085-1-5, 2016.

11. VON DREELE, R. B. Rietveld Refinement. In: **Powder Diffraction Theory and Practice**. Eds. DINNEBIER, R. E.; BILLINGE, S. L. Cambridge, UK, RSC Publishing. p. 58-88, 2008.

12. Bruker AXS, Topas v4.2, User's manual (2009).

13. BALZAR, D.; AUDEBRAND, N.; DAYMOND, M.; FITCH, A.; HEWAT, A.; LANGFORD, J. I.; LE BAIL, A.; LOUËR, D.; MASSON, O.; MCCOWAN, C. N.; POPA, N.C.; STEPHENS, P.W.; TOBY, B. Size-Strain Line-Broadening Analysis of the Ceria Round-Robin Sample. **J Appl Cryst**, v. 37, p. 911-924, 2004.

14. BALZAR, D. Voigt-function model in diffraction line-broadening analysis. In: **Microstructure Analysis from Diffraction**, International Union of Crystallography, 1999.

15. ICHIKAWA, R. U. Aplicações do método de Warren-Averbach de análise de perfis de difração. Dissertação de Mestrado em Tecnologia Nuclear – Materiais. Instituto de Pesquisas Energéticas e Nucleares, Universidade de São Paulo, São Paulo (2013).

16. GRZECHNIK, A.; NUSS, J.; FRIESE, K.; GESLAND, J.-Y.; JANSEN, M. Refinement of the crystal structure of potassium triyttrium decafluoride, KY_3F_{10}. **Z Kristallogr NCS**, v. 217, p. 460, 2002.

17. ICHIKAWA, R. U.; MARTINEZ, L. G.; IMAKUMA, K. TURRILLAS, X. Development of a methodology for the application of the Warren-Averbach method. In: **V ENCONTRO CIENTÍFICO DE FÍSICA APLICADA**, 2014, São Paulo. Annals. Blucher Physics Proceedings. n.1, v. 1. 2014. p. 107-110.

18. TEIXEIRA, M. I.; CALDAS, L. V. E. The influence of high doses of radiation in citrine stones. In: **INTERNATIONAL SYMPOSIUM ON SOLID STATE DOSIMETRY**, Cusco-Peru, April 13rd to 16th, pp. 391-399 (2014).